Development of organovermiculite-based adsorbent for removing anionic dye from aqueous solution

Xubiao Yu [a,c], Chaohai Wei [a,*], Lin Ke [a], Yun Hu [a], Xiaoqi Xie [a], Haizhen Wu [b]

[a] *College of Environmental Science & Engineering, South China University of Technology, Guangzhou, Guangdong 510006, PR China*
[b] *College of Bioscience & Bioengineering, South China University of Technology, Guangzhou, Guangdong 510006, PR China*
[c] *College of Chemical & Environmental Engineering, Liaoning University of Technology, Jinzhou, Liaoning 121001, PR China*

ARTICLE INFO

ABSTRACT

This paper reports on the development of organovermiculite-based adsorbent for removing Congo Red (CR), a model anionic dye, from aqueous solution. The organovermiculite was prepared using hexadecyl trimethylammonium bromide (HDTMAB) with variations in cation exchange capacity (CEC) and was then characterized by X-ray diffraction (XRD), Fourier transform infrared spectroscopy (FTIR), and scanning electron microscopy (SEM). The results from the adsorption experiments showed that with the organic modification of 50, 100, and 200% CEC, the adsorption capacity of vermiculite towards CR was greatly improved from 2.6 to 74.07, 175.44 and 192.31 mg/g, respectively, at 298 K. The adsorption isotherm experiment was conducted at different temperatures (298, 308 and 318 K), and it was found that the uptake of CR increased with increasing temperature. Langmuir and Freundlich isotherm models were applied and the Langmuir model was found to fit the equilibrium data better. The adsorption kinetics was found to follow the pseudo-second-order model. In addition, various thermodynamic parameters such as changes in enthalpy, entropy, and the Gibbs free energy were calculated, showing adsorption to be an endothermic yet spontaneous process. The results indicated that the organovermiculite may be an effective adsorbent for the removal of anionic dyes from wastewater.

© 2010 Elsevier B.V. All rights reserved.

1. Introduction

Dyes and pigments as additive materials have been widely used in many industries such as textiles, rubber, paper, and plastics. Recently, over 7×10^5 tons of dyes and pigments are produced annually, of which more than 10% of them persist in the waste effluents of these industries [1]. Because the disposal of these effluents into the receiving water body may cause severe damage to aquatic biota and humans due to mutagenic and carcinogenic effects [2], it is of great importance to provide waste-treatment facilities for minimizing these substances in the effluents before discharge.

Although there are several techniques available for treatment of dye-containing wastewater, such as biodegradation, chemical oxidation, photo degradation and electrochemical degradation, most of these are not very effective. The main reason is because the dye substances have complex aromatic structures which provide them with physico-chemical, thermal and optical stability [3], and with resistance to many chemicals, oxidizing agents, heat and biodegra-

dation [3,4]. The adsorption technique has been found not only to be effective, but also practical in application for the dye-containing wastewater treatment because of its high efficiency, simplicity, and the availability of a wide range of adsorbents [5,6]. Among the adsorbents, activated carbon is the most commonly used adsorbent for removing dyes from aqueous solutions. However, due to the cost, its application for a large-scale wastewater treatment is still limited. Exploitation of inexpensive and effective alternatives to activated carbon for the removal of dyes from wastewater has been the focus of intense research, of which clay minerals have become a strong candidate because of their abundance in the environment, wide distribution, low cost and high adsorption properties.

Clay materials mostly possess a layered structure and are considered as host materials [7]. Clay minerals applied in the adsorption of dyes from solution consist of two types: natural clays and organically modified clays (organoclay). For the natural clay, the negative charge of structure gives it the capability to adsorb positively charged species by the replacement of the exchangeable cations in the interlayer. Much work has been carried out on the adsorption of various cationic dyes such as methylene blue [7,8], malachite green [9], yellow 4GL [10,11], red GRL [12], and C.I. Basic Blue 41 [13] by different natural clays. However, the natural clay usually has a low adsorption capacity for anionic dyes due to the lack of effective adsorption sites. The organoclay is a

very important application of clay minerals and has been widely used as adsorbents of organic pollutants in soil, water and air. Ion exchange with alkylammonium ions is a well-known and preferential method for the preparation of organoclays [14]. An interesting phenomenon has been observed that organic modification can significantly improve the clay's adsorption capability towards anionic dyes. However, investigations on the adsorption mechanism of this process are relatively scarce. At present, the main mechanism proposed is believed to be the binding between anionic groups (e.g., sulfonic groups) of the dye and the positively charged surface of organoclays [15,16]. The adsorption mechanism is related to the preparation of organoclays, which include the optimum loading and choice of organic modifier. Recent research about the adsorption of anionic dyes on organoclays rarely deals with the effect of the loading of organic cations on the dye's removal.

Vermiculite, a kind of 2:1-type clay mineral expressed as $M_x(Al_{2-y}Fe_4^{3+})(Si_{4-x}Al_x)O_{10}(OH)_2 \cdot nH_2O$ (dioctahedral) or $M_x(Mg_3)(Si_{4-x}Al_x)O_{10}(OH)_2 \cdot nH_2O$ (trioctahedral) [17], is very abundant in China, and has mostly been used as a low-cost material for construction, refractory, soil amendment and so on. The utilization of vermiculite as an adsorbent material to replace activated carbon will greatly reduce costs in wastewater treatment. However, until now there are few studies on the organovermiculite-based adsorbent applied to dye-containing wastewater treatment.

In this work, we have conducted research on the natural vermiculite modification using hexadecyl trimethylammonium bromide (HDTMAB). Congo Red (CR), a typical anionic dye, was used as a model dye for evaluating the effectiveness of the modified vermiculite on the dye adsorption. The effects of other parameters such as temperature and time on the dye adsorption were also investigated. The objectives of this study were to (1) characterize the adsorption kinetics and isotherms of CR from aqueous solution onto organovermiculite, and (2) evaluate the relationship between organic loading and adsorption capacity.

2. Materials and methods

2.1. Materials and adsorbate

Vermiculite used in this study was supplied by DingSheng Mining Company from Shijiazhuang, Hebei Province, China. The raw vermiculite was treated before use. Vermiculite was mixed with deionised water at the ratio of 1:25 (vermiculite/water), was and then stirred at 150 rpm for 2 h. After 10 min of sedimentation, the suspension was discarded to remove unwanted materials such as fine particles and some soluble salts. The washing was repeated until the suspension became clear. The solid sample was dried at 105 °C for 24 h, and was then ground using an agate mortar to allow passage through a 200-mesh sieve. The fraction of particles between 0 and 75 μm was used in further experiments and designated as original vermiculite (OV). The CEC of vermiculite was determined as 102.7 mmol/100 g by the ammonium acetate method [18].

CR (C.I. 22120; chemical formula, $C_{32}H_{22}N_6Na_2O_6S_2$; molecular weight, 696.69) was obtained from Sigma–Aldrich. The chemical structure and molecular size of CR are illustrated in Fig. 1. All chemicals used were of analytical reagent grade.

2.2. Preparation of organovermiculite

The organocvermiculite was prepared by exchanging the inorganic cation of vermiculite with $HDTMA^+$ at 50, 100 and 200% of the clay's CEC. The quantity of organic cation added to the vermiculite

was determined by

$$f = \frac{M_{cation}}{CEC \cdot M_{clay} \cdot GMW_{cation} \cdot Z} \quad (1)$$

where f is the fraction of CEC satisfied by the organic cation (dimensionless), M_{cation} is the mass of organic cation required to achieve the desired fraction of CEC (mass), CEC is the cation exchange capacity of clay (equivalents/mass), M_{clay} is the clay mass, GMW_{cation} is the gram molecular weight of organic cation (mass/mol) and Z is the moles of charge per equivalent = 1 mol/equiv. for the cations used in this study (mol/equiv.) [19].

The synthesis of organovermiculite was performed as follows: 4 g of OV was first dispersed in 100 mL of deionised water, to which a desired amount of HDTMAB was slowly added. The suspensions were kept under agitation in a shaking table for 24 h at 40 °C, followed by a centrifugation of suspension at 4500 rpm for 15 min at room temperature. The samples were repeatedly washed by deionised water until AgNO₃ test for bromide anions showed negative. The washed organovermiculites were freeze-dried, ground and kept in a dry and dark place. They were designated as 50, 100 and 200 HDTMA.

2.3. Characterization

To determine the existence of organic functional groups, FTIR spectras of adsorbents were recorded on a Nicolet 6700 spectrometer (ThermoNicolet, USA) in the 4000–400 cm⁻¹ region using KBr platelets. The XRD analysis was performed using a D8 Advance X-ray power diffractometer (Bruker, Germany) with Cu Kα (λ = 1.5406 Å) radiation, scanning from 1° to 25° with a 2θ step of 0.021° and a step time of 1 s at 40 kV and 30 mA. The surface images of samples were examined using a JSM-6330F field emission SEM (JEOL, Japan). Gold was used as conductive material for samples coating.

2.4. Adsorption study

2.4.1. Sorption isotherm

Batch equilibrium studies were carried out by adding a weighed amount of organovermiculite (25 mg) into 100-ml conical flasks containing 25 ml of different initial concentration of CR solutions. The conical flasks were shaken at 170 rpm in a water bath at 298, 308 and 318 K. Control flasks without adsorbents were run in parallel to correct for possible removal of dyes by other mechanisms than adsorption. After shaking for 24 h, the adsorbents were separated by centrifugation at 4500 rpm for 10 min. The initial and equilibrium CR concentrations were determined by absorbance measurement using a Unico 2100 UV/vis spectrophotometer (Unico, China) at 498 nm. It was then computed to CR concentrations using a standard calibration curve. The amount of adsorption at equilibrium, q_e (mg/g), was calculated by

$$q_e = \frac{(C_0 - C_e) \cdot V}{W} \quad (2)$$

where C_0 and C_e (mg/L) are the liquid-phase concentrations of CR at initial and equilibrium states, respectively. V (L) is the volume of the solution and W (g) is the mass of adsorbent used.

2.4.2. Kinetic studies

The kinetics of dye adsorption on organovermiculite was studied by equilibrating 25 mg adsorbents with 25 mL CR solutions (92.9 mg/L) at different time intervals. After equilibration, organovermiculite was separated from the solution by centrifugation at 4500 rpm for 10 min and dyes residues were quantified in the supernatant. The amount of dye adsorbed by the organovermiculite was calculated as mentioned above.
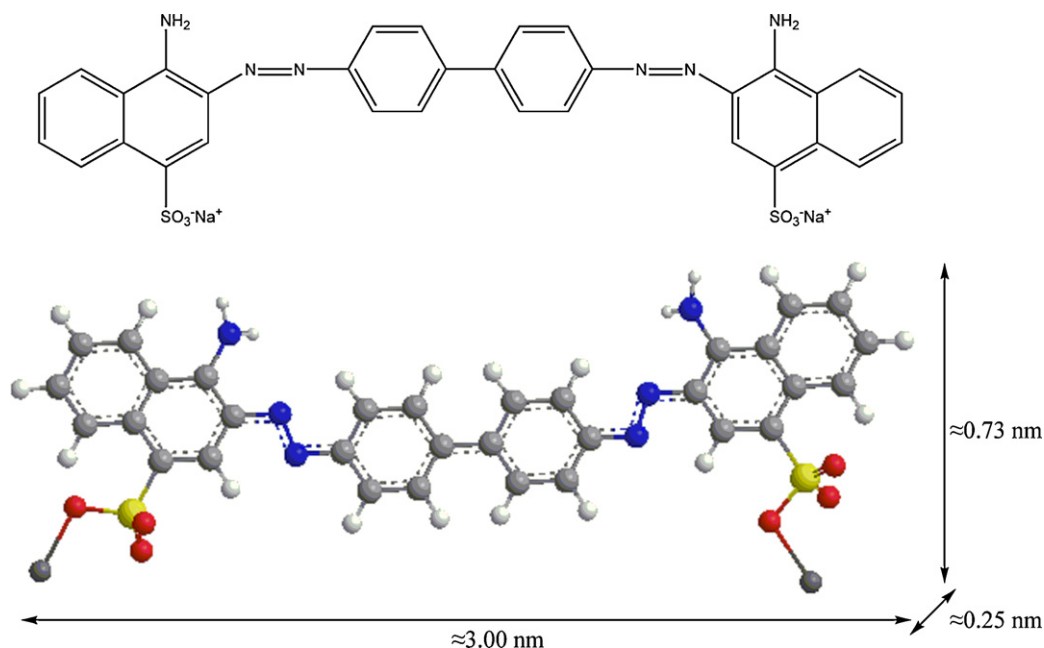
Fig. 1. Molecular structure and estimated molecular size of Congo Red.

3. Results and discussion

3.1. Characterization

3.1.1. FTIR

FTIR spectroscopy presents a useful tool to initially confirm the interaction between HDTMA+ and vermiculite. The FTIR spectra of OV and organovermiculite are shown in Fig. 2. The spectrum of OV shows bands at 3567 and 1010 cm^{-1} identified as O–H stretching vibrations of Si–OH groups [20] and Si–O–Si groups of the silicate layers [21], respectively. The band at 3423 cm^{-1} corresponds to the –OH vibration of the tetrahedral sheets [22]. It can be seen that those bands related to the structural characteristics of vermiculite remained nearly unchanged after the organic modification. The bands at 719, 684 and 458 cm^{-1} correspond to the deforma-

Fig. 2. FTIR spectra of OV and organovermiculite.

tion and bending modes of the Si–O [23]. After intercalating with HDTMA+, these bands had shifted to 721, 688 and 458 cm^{-1} at 50 HDTMA, 721, 692 and 459 cm^{-1} at 100 HDTMA, and 721, 694 and 457 cm^{-1} at 200 HDTMA. The bands of the characteristic stretching vibration of the –CH$_2$ (2850 cm^{-1}) and –CH$_3$ (2919 cm^{-1}), and the bending vibration of –CH$_3$ (1467 cm^{-1}) were observed on the spectra of organovermiculites. This suggests that the HDTMA+ had been loaded on the vermiculite. It is notable that with the increase of organic loading from 100 to 200% CEC, the absorption bands of –CH$_2$ and –CH$_3$ had few changes. This may indicate that the exchange between HDTMA+ and the exchangeable cations approached an equilibrium [24,25]. The absorption at 1637 cm^{-1} was primarily due to water directly coordinated to the exchangeable cations of the clay [26]. It can be seen from the spectra that this band weakened with the increase of HDTMA+. Therefore, this phenomenon is a good indication of the replacement of the interlayer cations with the HDTMA+. Moreover, the property of the silicate layer has been changed from hydrophilic to hydrophobic.
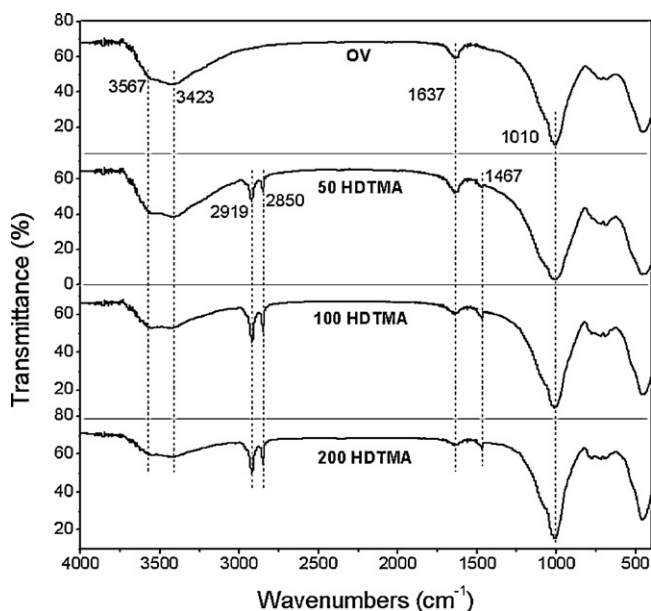
3.1.2. XRD

The XRD patterns of OV and organovermiculites are presented in Fig. 3. For OV, the peak at 2θ 5.93° gives the characteristic basal spacing (d_{001}) of 1.49 nm for vermiculite. The peak at 2θ 7.99° indicates the impurities of mica mineral presented in the vermiculite. At 50 HDTMA, the peak at 2θ 5.93° ($d = 1.49$ nm) weakened and a new peak appeared at 2θ 3.17° ($d = 2.78$ nm); here, the HDTMA+ may lie flat on the silicate surface as a monolayer or bilayer because of the low concentration of HDTMA+ [14]. When the loading of HDTMAB increased to 100% CEC, the peak at 2θ 5.93° further weakened and a strong new peak appeared at 2θ 1.69° ($d = 5.23$ nm) as a result of the increment of the HDTMA ions. The adsorbed HDTMA+ mainly formed a paraffin [27] or an admicelle [28] structure, and small amounts of monolayer/bilayer ($d = 2.87$ nm) and original vermiculite structures ($d = 1.41$ nm) were still present. For the 200 HDTMA, the peaks at 2θ 5.93° and 2θ 3.17° all disappeared and the peak at 2θ 1.69° appeared sharper and more defined. The paraffin or admicelle structure became the exclusive structure. Compared to other reported organoclays such as the organobentonite, the organovermiculites prepared in this study presented a large increase in the basal spacing. For organic ions such as
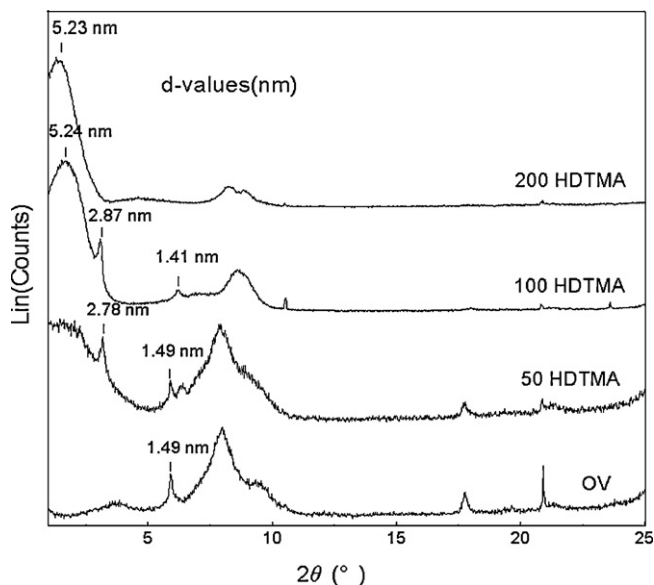
Fig. 3. X-ray diffraction patterns of OV and organovermiculite.

HDTMA+, there is a high dependence of the interlayer space structure on the surface charge density of the clay mineral and higher charges of the vermiculite can lead to greater basal spacing than in the case of smectite [28]. Therefore, the greater basal spacing of the organovermiculite in the present study might indicate that more HDTMA+ had been offered in the exchange solution.

3.1.3. SEM

The comparative changes in the texture of clay materials are given in the SEM images presented in Fig. 4. For OV, typical arrangements of silicate mineral platelets were clearly seen (Fig. 4a and

b). After the intercalation of HDTMA+, it can be observed that the lamellar structure was loosened and a rougher surface was obtained (Fig. 4c and d).

3.2. Adsorption kinetics

Adsorption kinetics, demonstrating the uptake rate of pollutants, is one of the most important characteristics representing the adsorption efficiency of organovermiculite. Fig. 5 shows the adsorption kinetics of CR by organovermiculites and OV at the initial dye concentration of 92.9 mg/L. It can be found that OV had a weak affinity towards CR; this result is similar to the report about the adsorption of an acid dye onto hectorite [29]. The possible reason may be that the negatively charged surface of the clay cannot provide effective adsorption sites for dye anions. After organic modification, the adsorption capability was enhanced greatly and the removal of CR was 77, 92 and 99% for 50, 100 and 200 HDTMA,
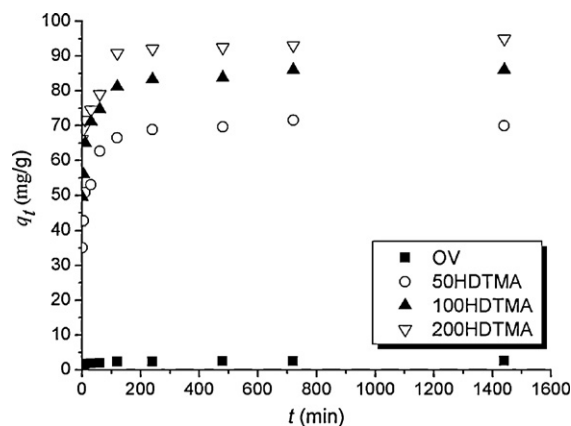

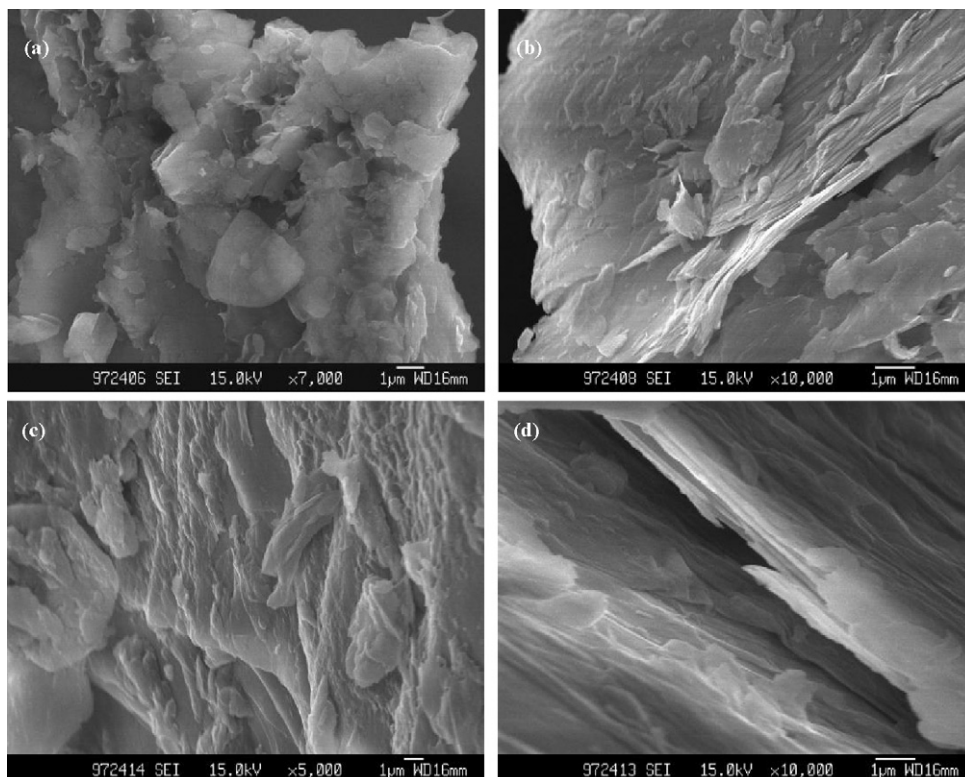**Fig. 5.** Effect of contact time on the adsorption of CR.

Fig. 4. SEM images for OV (a and b) and organovermiculite (100 HDTMA) (c and d).
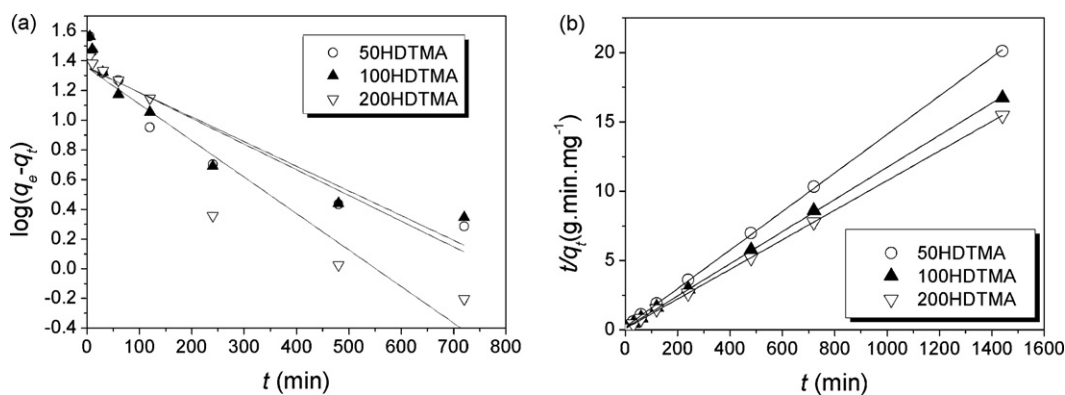
Fig. 6. Pseudo-first-order (a) and pseudo-second-order (b) kinetic models for the adsorption of CR onto organovermiculite.

respectively. It was also found that the adsorption rates increased dramatically in the initial stages of the sorption process for the organovermiculites. The adsorption capacity for the first hour of contact was found to reach 76.1, 81.3 and 81.2% of the total uptake for 50, 100 and 200 HDTMA, respectively.

To further elucidate the CR adsorption kinetics over organovermiculite, the adsorption data were examined by the pseudo-first-order [30] and pseudo-second-order [31] kinetic models, given in Eqs. (3) and (4), respectively:

$$\log(q_e - q_t) = \log(q_e) - \frac{k_1}{2.303}t \tag{3}$$

$$\frac{t}{q_t} = \frac{1}{k_2 q_e^2} + \frac{1}{q_e}t \tag{4}$$

where k_1 (1/min) and k_2 (g/mg min) are the rate constants of pseudo-first-order and pseudo-second-order kinetic models, respectively; q_t and q_e are the amount of dye adsorbed (mg/g) at contact time t (min) and equilibrium, respectively. As shown in Fig. 6(a), the pseudo-first-order model for CR adsorption exhibited a poor linear relationship, suggesting that CR adsorption on organovermiculite did not follow this model well. In contrast, in Fig. 6(b), the plots of t/q_t versus time t resulted in very high correlation coefficients ($R^2 > 0.99$), indicating good compliance with the pseudo-second-order equation for CR adsorption onto organovermiculite. Moreover, the values of the rate constants and the calculated q_e values are shown in Table 1. It can be found that the calculated q_e values by the pseudo-second-order model were very close to those of the experimentally obtained q_e, further confirming that the adsorption of CR on organovermiculite obeyed the pseudo-second-order kinetic model.

The original pseudo-second-order kinetic models can be expressed as [32]:

$$\frac{d(q_t/q_e)}{dt} = k_2 q_e \left[1 - \left(\frac{q_t}{q_e}\right)\right]^2 \tag{5}$$

In this equation, $k_2 q_e$ can be defined as the second-order rate index which can reflect the kinetic performance [32]. The $k_2 q_e$ value is equal to the inverse of the half-life of the adsorption process and is proportional to the adsorption rate. It can be found from Table 1 that the value of $k_2 q_e$ has the following order: 100 HDTMA > 50 HDTMA > 200 HDTMA. With the same CR concentration (i.e., the same diffusion potential), the adsorption rate of CR is dependent on the amount of adsorption sites and the pore structure of adsorbents. With the increase of organic loading, the adsorption sites of organovermiculites were increased (it will be further discussed in Section 3.5); however, the excessive HDTMA$^+$ can also occupy or block the pore channel of the adsorbents (as 200 HDTMA) [33–35], which will hinder the diffusion of CR molecules. Therefore, by possessing sufficient adsorption sites and un-blocked pore channels, the sample of 100 HDTMA exhibits a larger adsorption rate than the others in this study.

3.3. Adsorption isotherms

The adsorption isotherms for CR on organovermiculite at three temperatures (T = 298, 308 and 318 K) are shown in Fig. 7. It is evident that the uptake of CR on organovermiculite increased with temperature. The batch adsorption experimental data are fitted to the Langmuir and Freundlich isotherm models.

The Langmuir model assumes that the uptake of adsorbate occurs on a homogeneous surface by monolayer without any interaction between the adsorbed molecules. The linear form of the Langmuir equation can be expressed as [36]:

$$\frac{C_e}{q_e} = \frac{1}{q_m K_L} + \frac{C_e}{q_m} \tag{6}$$

where q_m (mg/g) and K_L (L/mg) are the Langmuir constants related to the maximum adsorption capacity and energy of adsorption, respectively. The plot of C_e/q_e versus C_e gives a straight line at each temperature, confirming that the Langmuir isotherm is followed in the adsorption process. The values of calculated parameters for Langmuir are presented in Table 2.

As an important parameter, q_m has been shown to evaluate the adsorption capacity of CR in many studies. Table 3 summarizes the comparison of CR adsorption capacities by various types of adsorbents used in the recent literature. The performance shown by organovermiculite (200 HDTMA) was suitable as compared to other adsorbents, reflecting a promising future for vermiculite utilization in wastewater treatment applications.

Table 1
Parameters of the pseudo-first-order and pseudo-second-order kinetic models.

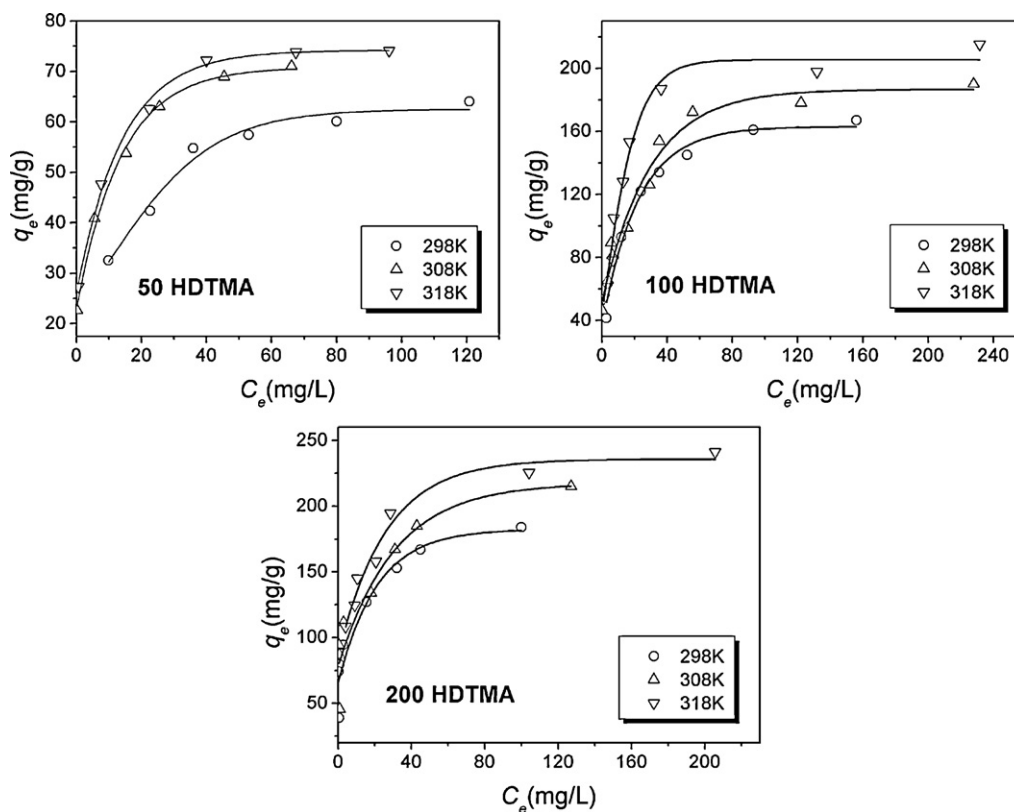| Adsorbents	$q_{e,exp}$ (mg g^{-1})	Pseudo-first-order model			Pseudo-second-order model			
		k_1 ($\times 10^3$ min^{-1})	$q_{e,cal}$ (mg g^{-1})	R^2	k_2 ($\times 10^3$ g mg^{-1} min^{-1})	$q_{e,cal}$ (mg g^{-1})	$k_2 q_{e,cal}$ ($\times 10^3$ min^{-1})	R^2
50 HDTMA	71.65	3.9	22.77	0.878	1.9	70.42	133.80	0.999
100 HDTMA	86.45	3.9	22.52	0.866	8.6	87.49	752.41	0.999
200 HDTMA	93.12	5.8	22.56	0.918	1.3	92.59	120.37	0.999

Fig. 7. Adsorption isotherms of CR onto organovermiculite at different temperatures.

Table 2
Isotherm parameters for adsorption of CR onto organovermiculite.

Adsorbent	T (K)	Langmuir				Freundlich		
		q_m (mg/g)	K_L (L/mg)	R_L	R^2	K_F (L/mg)	n	R^2
50 HDTMA	298	74.07	0.09	0.069	0.997	18.23	3.62	0.931
	308	74.07	0.28	0.036	0.994	30.85	4.89	0.990
	318	76.92	0.31	0.030	0.998	31.27	4.83	0.980
100 HDTMA	298	175.44	0.10	0.031	0.999	37.83	3.05	0.920
	308	196.08	0.11	0.034	0.996	57.90	4.31	0.941
	318	222.22	0.12	0.021	0.998	58.16	3.72	0.887
200 HDTMA	298	192.31	0.16	0.013	0.994	72.74	4.82	0.808
	308	227.27	0.11	0.017	0.991	81.85	5.00	0.757
	318	250.00	0.12	0.017	0.999	84.16	4.75	0.941

Table 3
The maximum adsorption capacity (q_m) for CR of various adsorbents.

Adsorbent	q_m (mg/g)	T (K)	R^2	Reference
Bottom ash	0.14	303	–	[37]
Deoiled soya	1.08	303	–	[37]
Australian kaolins	7.27	303	0.991	[38]
Na-bentonite	35.84	303	0.973	[39]
Perlite	55.55	303	0.993	[3]
Marine Alga *Porphyra yezoensis Ueda*	71.46	298	0.995	[40]
N,O-carboxymethyl-chitosan/montmorillonite	74.24	303	–	[41]
Ca-bentonite	107.41	293	0.978	[42]
Organovermiculite (200 HDTMA)	192.31	298	0.994	This work
Chitosan hydrogel	208.1	303	0.997	[43]
Maghemite nanoparticles	208.33	298	0.998	[44]
Chitosan hydrogel beads impregnated with carbon nanotubes	450.4	303	0.998	[45]

The essential characteristics of the Langmuir isotherm can be expressed by a dimensionless constant called equilibrium parameter R_L [46], defined by

$$R_L = \frac{1}{1 + K_L C_0} \qquad (7)$$

where C_0 (mg/L) is the highest dye concentration. The value of R_L indicates whether the type of isotherm will be unfavorable ($R_L > 1$), linear ($R_L = 1$), favorable ($0 < R_L < 1$) or irreversible ($R_L = 0$). As shown in Table 2, the calculated values of R_L are between 0 and 1. This implies that the adsorption of CR on organovermiculite was favorable under the conditions studied.

The Freundlich model assumes a heterogeneous adsorption surface having unequally available sites with different energies of adsorption. The linear form of the Freundlich equation can be expressed as [47]:

$$\ln q_e = \ln K_F + \frac{1}{n} \ln C_e \qquad (8)$$

where K_F (L/mg) and n are the Freundlich constants incorporating all the factors, such as adsorption capacity and adsorption intensity, affecting the adsorption process. The parameters calculated by the fitting of $\ln q_e$ versus $\ln C_e$ are shown in Table 2. It can be seen that the correlation coefficients (R^2) of the Freundlich model are lower than those of the Langmuir model, thus Langmuir model is the better fit model for the adsorption of CR onto organovermiculite.

3.4. Adsorption thermodynamics

The thermodynamic parameters are important for a better understanding of the effect of temperature on adsorption [48]. The thermodynamic parameters such as Gibbs free energy ($\Delta G°$), standard enthalpy ($\Delta H°$) and standard entropy ($\Delta S°$) of the adsorption processes were obtained from the adsorption experiments at various temperatures (298, 308 and 318 K) and were estimated using Eqs. (9)–(11) [49]:

$$K_c = \frac{C_{Ad}}{C_e} \qquad (9)$$

$$\Delta G° = -RT \ln K_c \qquad (10)$$

$$\log K_c = \frac{\Delta S°}{2.303R} - \frac{\Delta H°}{2.303RT} \qquad (11)$$

Table 4
Thermodynamic parameters for adsorption of CR onto organovermiculite.

Sample	$\Delta H°$ (kJ/mol)	$\Delta S°$ (J/mol K)	$\Delta G°$ (kJ/mol)			R^2
			298 K	308 K	318 K	
50 HDTMA	4.76	16.44	−1.22	−2.31	−3.97	0.985
100 HDTMA	8.84	31.57	−4.78	−7.08	−10.05	0.993
200 HDTMA	4.72	20.66	−11.90	−13.70	−15.33	0.999
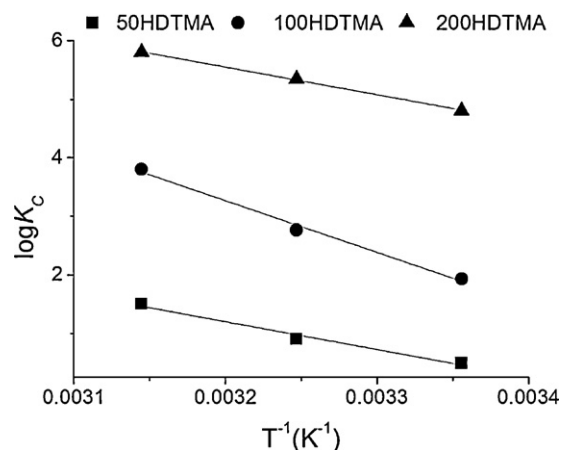
Fig. 8. Van't Hoff plot for the CR adsorption onto organovermiculite.

where K_c is the equilibrium constant, C_{Ad} (mg/L) is the concentration of CR on solid at equilibrium, C_e is the equilibrium concentration of CR in solution, R is the gas constant (8.314 J/kmol) and T is the temperature (K). The values of $\Delta S°$ and $\Delta H°$ were determined from the slopes and intercepts of the Van't Hoff plot of $\log K_c$ versus $1/T$ (Fig. 8). The use of the Van't Hoff plot is an indirect method to calculate thermodynamic adsorption parameters at solid/liquid interface [50]. The thermodynamic parameter values are shown in Table 4.

The negative values of $\Delta G°$ indicate the feasibility of the process and spontaneous nature of adsorption. The value of $\Delta G°$ became more negative with increasing temperature for all adsorbents. This suggests that an increase in temperature was favorable for the CR removal process. The positive value of $\Delta H°$ confirms the endothermic nature of the adsorption process. The positive value of $\Delta S°$
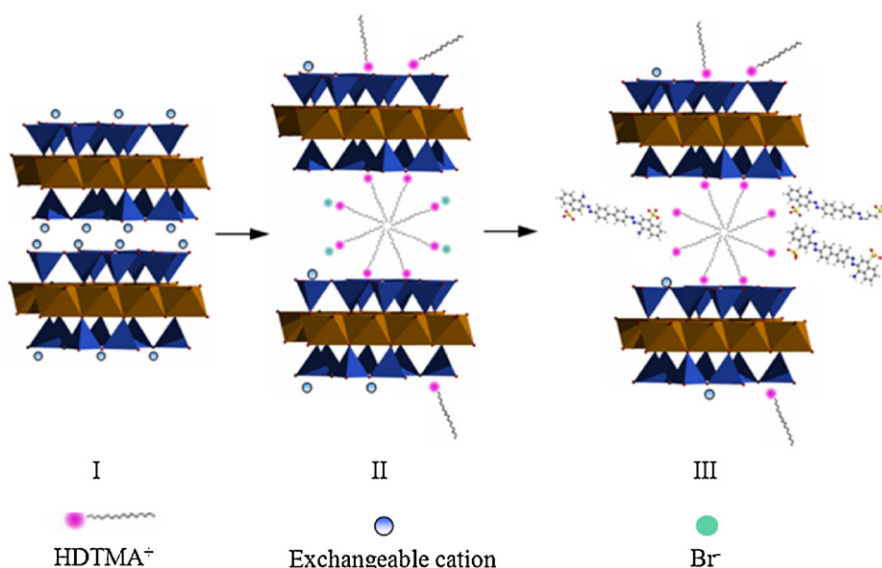

Fig. 9. Suggested structures of CR adsorption onto organovermiculite: I, OV; II organovermiculite (has a micelle-type structure); III, adsorption of CR onto organovermiculite.

corresponded to an increased degree of freedom in the system as a result of adsorption.

3.5. Effect of HDTMA⁺ loading on CR adsorption

When used in applications, the organic loading is an important parameter for preparing organoclays and the optimum loading should be determined before use. The effects of HDTMA⁺ loading on CR uptake at three temperatures can be evaluated from Table 2. Due to a high correlation with the Langmuir model, the parameter of q_m was used to evaluate the adsorption capacity of CR. The q_m was found to increase greatly with increasing HDTMA⁺ loading from 0 to 100% CEC at different temperatures. This phenomenon can be attributed to the increase of exchangeable anions in the organovermiculite. It has been reported that paraffin-type and micelle-type are the main possible arrangements of alkylammonium ions intercalated in clay minerals. In these pillared structures, besides the uptake of organic cations, the organic molecules could also be adsorbed by the attraction between long chain alkyls, such that the halide ions give the organoclay an anionic exchange capacity. Several papers have reported this character of organoclay. Bors et al. [51] studied the sorption of anionic radionuclides on organoclays, where the sorption capabilities were found to increase with increasing contents of organic cations. Zhu and Ma [15] studied the removal of orange II (an anionic dye) and HDTMAB by bentonite in one step, he pointed out that Orange II was adsorbed mainly due to the anionic exchange with Br⁻ of the adsorbed CTMAB in the interlayer of bentonite. In our study, with the organic loading increasing from 0 to 100% CEC, the CR uptake showed an obvious increase due to the increase of HDTMAB in the interlayer. For better illustration of the process of adsorption, a suggested adsorption structure is shown in Fig. 9.

However, increasing the loading from 100 to 200% CEC shows only a small increase in the uptake of CR. This suggests that the intercalation of HDTMAB into the interlayers is more difficult when the loading is above 100% CEC as the adsorption reached equilibrium. This phenomenon is consistent with the result obtained from FTIR. For application initiatives, the loading of 100% CEC is more cost-effective than that of 200% CEC for the removal of CR.

4. Conclusions

This study investigated the dynamics and equilibrium of the adsorption of Congo Red onto organvermiculite modified by HDTMAB. The effectiveness of the intercalation process was clearly demonstrated by the characterization methods of FTIR, XRD and SEM. The adsorption capacities of 50 HDTMA, 100 HDTMA and 200 HDTMA were 27.5, 66.5 and 73.0 times higher than that of the natural vermiculite at 298 K, respectively. The adsorption capacities were increased greatly with increasing HDTMAB from 0 to 100% CEC, but quickly leveled off from 100 to 200% CEC. The kinetic experimental result shows that it followed the pseudo-second-order kinetic model. The adsorption isotherms were well fit by the Langmuir model. The calculation of the thermodynamic parameters indicates that CR adsorption onto organovermiculite was endothermic and spontaneous in nature. Overall, the high adsorption capacity and rapid adsorption rate of organovermiculite suggest that it could be used as an effective adsorbent for the removal of anionic dyes from wastewater.

References

[1] T. Deveci, A. Unyayar, M.A. Mazmanci, Production of remazol brilliant Blue R decolourising oxygenase from the culture filtrate of funalia trogii ATCC 200800, J. Mol. Catal. A-Enzym. 30 (2004) 25–32.

[2] G. Crini, Non-conventional low-cost adsorbents for dye removal: a review, Bioresour. Technol. 97 (2006) 1061–1085.

[3] G. Vijayakumar, M. Dharmendirakumar, S. Renganathan, S. Sivanesan, G. Baskar, K.P. Elango, Removal of congo red from aqueous solutions by perlite, Clean – Soil Air Water 37 (2009) 355–364.

[4] V.K. Gupta, Suhas, Application of low-cost adsorbents for dye removal—a review, J. Environ. Manage. 90 (2009) 2313–2342.

[5] S. Chatterjee, D.S. Lee, M.W. Lee, S.H. Woo, Enhanced adsorption of congo red from aqueous solutions by chitosan hydrogel beads impregnated with cetyl trimethyl ammonium bromide, Bioresour. Technol. 100 (2009) 2803–2809.

[6] D. Karadag, M. Turan, E. Akgul, S. Tok, A. Faki, Adsorption equilibrium and kinetics of reactive black 5 and reactive red 239 in aqueous solution onto surfactant-modified zeolite, J. Chem. Eng. Data 52 (2007) 1615–1620.

[7] Y.E. Mouzdahir, A. Elmchaouri, R. Mahboub, A. Gil, S.A. Korili, Adsorption of methylene blue from aqueous solutions on a moroccan clay, J. Chem. Eng. Data 52 (2007) 1621–1625.

[8] S. Hong, C. Wen, J. He, F. Gan, Y.S. Ho, Adsorption thermodynamics of methylene blue onto bentonite, J. Hazard. Mater. 167 (2009) 630–633.

[9] S.S. Tahir, N. Rauf, Removal of a cationic dye from aqueous solutions by adsorption onto bentonite clay, Chemosphere 63 (2006) 1842–1848.

[10] A.A. Futaisi, A. Jamrah, R.A. Hanai, Aspects of cationic dye molecule adsorption to palygorskite, Desalination 214 (2007) 327–342.

[11] E. Eren, B. Afsin, Investigation of a basic dye adsorption from aqueous solution onto raw and pre-treated sepiolite surfaces, Dyes Pigments 73 (2007) 162–167.

[12] M. Doğan, M. Hamdi Karaoğlu, M. Alkan, Adsorption kinetics of maxilon yellow 4GL and maxilon red GRL dyes on kaolinite, J. Hazard. Mater. 165 (2009) 1142–2115.

[13] M. Roulia, A.A. Vassiliadis, Interactions between C.I. Basic Blue 41 and aluminosilicate sorbents, J. Colloid Interface Sci. 291 (2005) 37–44.

[14] L.B. de Paiva, A.R. Morales, F.R.V. Díaz, Organoclays: properties, preparation and applications, Appl. Clay Sci. 42 (2008) 8–24.

[15] L. Zhu, J. Ma, Simultaneous removal of acid dye and cationic surfactant from water by bentonite in one-step process, Chem. Eng. J. 139 (2008) 503–509.

[16] M. Pulikesi, V. Ramamurthi, S. Sivanesan, Equilibrium studies for the adsorption of Acid dye onto modified hectorite, J. Hazard. Mater. 136 (2006) 989–992.

[17] T. Shichi, K. Takagi, Clay minerals as photochemical reaction fields, J. Photochem. Photobiol. C 1 (2000) 113–130.

[18] A. Vazquez, M. López, G. Kortaberria, L. Martín, I. Mondragon, Modification of montmorillonite with cationic surfactants. Thermal and chemical analysis including CEC determination, Appl. Clay Sci. 41 (2008) 24–36.

[19] B. Zohra, K. Aicha, S. Fatima, B. Nourredine, D. Zoubir, Adsorption of Direct Red 2 on bentonite modified by cetyltrimethylammonium bromide, Chem. Eng. J. 136 (2008) 295–305.

[20] E.J. Acosta, Y. Deng, G.N. White, J.B. Dixon, K.J. McInnes, S.A. Senseman, A.S. Frantzen, E.E. Simanek, Dendritic surfactants show evidence for frustrated intercalation: a new organoclay morphology, Chem. Mater. 15 (2003) 2903–2909.

[21] C.J. Liao, C.P. Chen, M.K. Wang, P.N. Chiang, C.W. Pai, Sorption of chlorophenoxy propionic acids by organoclay complexes, Environ. Toxicol. 21 (2006) 71–79.

[22] T.S. Anirudhan, P.S. Suchithra, S. Rijith, Amine-modified polyacrylamide–bentonite composite for the adsorption of humic acid in aqueous solutions, Colloids Surf. A 326 (2008) 147–156.

[23] V.C. Farmer, The Infrared Spectra of Minerals, Minerological Society, London, 1974.

[24] D. Plachá, G.S. Martynková, M.H. Rümmeli, Preparation of organovermiculites using HDTMA: structure and sorptive properties using naphthalene, J. Colloid Interface Sci. 327 (2008) 341–347.

[25] S. Changchaivong, S. Khaodhiar, Adsorption of naphthalene and phenanthrene on dodecylpyridinium-modified bentonite, Appl. Clay Sci. 43 (2009) 317–321.

[26] P. Kulshrestha, R.F. Giese Jr., D.S. Aga, Investigating the molecular interactions of oxytetracycline in clay and organic matter: insights on factors affecting its mobility in soil, Environ. Sci. Technol. 38 (2004) 4097–4105.

[27] H.O. Assmann, M.B. Zayani, S. Geiger, B. Fraisse, N.K. Ariguib, M.T. Ayadi, N.E. Ghermani, J.L. Grossiord, Physico-chemical characterizations of tunisian organophilic bentonites, J. Phys. Chem. C 111 (2007) 10869–10877.

[28] S. Dultz, B. Riebe, C. Bunnenberg, Temperature effects on iodine adsorption on organo-clay minerals. II. Structural effects, Appl. Clay Sci. 28 (2005) 17–30.

[29] P. Baskaralingam, M. Pulikesi, V. Ramamurthi, S. Sivanesan, Equilibrium studies for the adsorption of Acid dye onto modified hectorite, J. Hazard. Mater. 136 (2006) 989–992.

[30] S.K. Lagergren, About the theory of so-called adsorption of soluble substances, Sven. Vetenskapsakad. Handl. 24 (1898) 1–39.

[31] Y.S. Ho, G. McKay, Pseudo-second order model for sorption processes, Process Biochem. 34 (1999) 451–465.

[32] F. Wu, R. Tseng, S. Huang, R. Juang, Characteristics of pseudo-second-order kinetic model for liquid-phase adsorption: a mini-review, Chem. Eng. J. 151 (2009) 1–9.

[33] Z. Bouberka, A. Khenifi, H. Ait Mahamed, B. Haddou, N. Belkaid, N. Bettahar, Z. derriche, Adsorption of Supranol Yellow 4 GL from aqueous solution by surfactant-treated aluminum/chromium-intercalated bentonite, J. Hazard. Mater. 162 (2009) 378–385.

[34] A.M.F. Guimarães, V.S.T. Ciminelli, W.L. Vasconcelos, Smectite organofunctionalized with thiol groups for adsorption of heavy metal ions, Appl. Clay Sci. 42 (2009) 410–414.

[35] R. Zhu, L. Zhu, J. Zhu, F. Ge, T. Wang, Sorption of naphthalene and phosphate to the CTMAB–Al$_{13}$ intercalated bentonites, J. Hazard. Mater. 168 (2009) 1590–1594.

[36] I. Langmuir, The adsorption of gases on plane surface of glass, mica, and platinum, J. Am. Chem. Soc. 40 (1918) 1361–1403.

[37] A. Mittal, J. Mittal, A. Malviya, V.K. Gupta, Adsorptive removal of hazardous anionic dye "Congo red" from wastewater using waste materials and recovery by desorption, J. Colloid Interface Sci. 340 (2009) 16–26.

[38] V. Vimonses, S. Lei, B. Jin, C.W.K. Chow, C. Saint, Adsorption of congo red by three Australian kaolins, Appl. Clay Sci. 43 (2009) 465–472.

[39] V. Vimonses, S. Lei, B. Jin, C.W.K. Chow, C. Saint, Kinetic study and equilibrium isotherm analysis of Congo Red adsorption by clay materials, Chem. Eng. J. 148 (2009) 354–364.

[40] X.S. Wang, J.P. Chen, Removal of the azo dye Congo Red from aqueous solutions by the marine alga Porphyra yezoensis Ueda, Clean – Soil Air Water 37 (2009) 793–798.

[41] L. Wang, A. Wang, Adsorption behaviors of Congo red on the N,O-carboxymethyl-chitosan/montmorillonite nanocomposite, Chem. Eng. J. 143 (2008) 43–50.

[42] L. Lian, L. Guo, C. Guo, Adsorption of Congo red from aqueous solutions onto Ca-bentonite, J. Hazard. Mater. 161 (2009) 126–131.

[43] S. Chatterjee, T. Chatterjee, S.H. Woo, A new type of chitosan hydrogel sorbent generated by anionic surfactant gelation, Bioresour. Technol. 101 (2010) 3853–3858.

[44] A. Afkhami, R. Moosavi, Adsorptive removal of Congo red, a carcinogenic textile dye, from aqueous solutions by maghemite nanoparticles, J. Hazard. Mater. 174 (2010) 398–403.

[45] S. Chatterjee, M.W. Lee, S.H. Woo, Adsorption of congo red by chitosan hydrogel beads impregnated with carbon nanotubes, Bioresour. Technol. 101 (2010) 1800–1806.

[46] T.W. Webei, R.K. Chakravort, Pore and solid diffusion models for fixed-bed adsorbers, AIChE J. 20 (1974) 228–238.

[47] H.M.F. Freundlich, Over the adsorption in solution, J. Phys. Chem. 57 (1906) 385–470.

[48] C.A.P. Almeida, N.A. Debacher, A.J. Downs, L. Cottet, C.A.D. Mello, Removal of methylene blue from colored effluents by adsorption on montmorillonite clay, J. Colloid Interface Sci. 332 (2009) 46–53.

[49] A. Kamari, W.S.W. Ngah, Isotherm, kinetic and thermodynamic studies of lead and copper uptake by H$_2$SO$_4$ modified chitosan, Colloids Surf. B 73 (2009) 257–266.

[50] C.E. Zubieta, P.V. Messina, C. Luengo, M. Dennehy, O. Pieroni, P.C. Schulz, Reactive dyes remotion by porous TiO$_2$-chitosan materials, J. Hazard. Mater. 152 (2008) 765–777.

[51] J. Bors, S. Dultz, B. Riebe, Organophilic bentonites as adsorbents for radionuclides. I. Adsorption of ionic fission products, Appl. Clay Sci. 16 (2000) 1–13.